Santoro, Pablo; Huybrechts, Nicolas; Fossati, Mónica; van Bang, Damien Pham; Tassi, Pablo; Piedra-Cueva, Ismael

2D and 3D numerical study of the Montevideo Bay hydrodynamics and fine sediment dynamics

2D and 3D numerical study of the Montevideo Bay hydrodynamics and fine sediment dynamics

Pablo Santoro
Instituto de Mecánica de los Fluidos
e Ingeniería Ambiental
Universidad de la República
Montevideo, Uruguay
Email: psantoro@fing.edu.uy

Mónica Fossati
Instituto de Mecánica de los Fluidos
e Ingeniería Ambiental
Universidad de la República
Montevideo, Uruguay
Email: mfossati@fing.edu.uy

Pablo Tassi
Saint Venant Laboratory for Hydraulics
EDF R&D
Chatou, France
Email: pablo.tassi@edf.fr

Nicolas Huybrechts
Roberval Laboratory, LHN (UTC)
CEREMA
Compiègne, France
Email: nicolas.huybrechts@cerema.fr

Damien Pham Van Bang
Saint Venant Laboratory for Hydraulics
CEREMA
Chatou, France
Email: damien.pham-van-bang@cerema.fr

Ismael Piedra-Cueva
Instituto de Mecánica de los Fluidos
e Ingeniería Ambiental
Universidad de la República
Montevideo, Uruguay
Email: ismaelp@fing.edu.uy

***Abstract*—This work has two main objectives, firstly the effect of the consolidation process on the bed evolution and fine sediment dynamics of the Río de la Plata estuary are explored. Secondly, the implementation of a high resolution 3D wave-current-sediment transport model to simulate the flow field and sediment transport processes of the Río de la Plata estuary and more specifically at Montevideo Bay area. We used a previously implemented 2D wave-current-sediment transport model. The consolidation model was calibrated by settling column experiments results, and good agreement was found between measured vertical bed density profiles in the Montevideo Bay area and the model results. Regarding the second objective, it is presented here the main characteristics of the 3D model implementation and a sensitivity analysis to different hydrodynamics and sediment transport parameters. In particular it is analysed the model response under different erosion-deposition paradigms.**

I. Introduction

Montevideo Bay hosts the main port of Uruguay along with a large industrial development. Nowadays there are many maritime engineering projects in the area, including the construction of new breakwaters, land reclamation for container terminals, navigation channels deepening, etc. All these projects need a reliable characterization of the hydrodynamics in the area and also for some of them the sediment dynamics. Numerical modelling is a powerful tool in that sense, not only for the design of these projects but also to assess their impact on the whole area.

A two-dimensional depth-averaged circulation, wave, sediment transport and bed evolution model was successfully implemented for the Río de la Plata focusing on the Montevideo coastal area [22]. Based on the open source TELEMAC-MASCARET Modeling System (TMS), it was possible to address the simulation of both the tidal and wave hydrodynamics, fine sediment transport and bed evolution with a single code. Using a single mesh for all the modules (TELEMAC2D-TOMAWAC-SISYPHE), and taking advantage of its non-structured nature, it was possible to provide high-resolution results in areas of complex geometries. The model was calibrated and validated using data of sea surface elevation (SSE), currents, waves, and suspended sediment concentration (SSC) in several stations. The obtained results show good agreement with the measured data, representing satisfactorily the main features of the Río de la Plata dynamics [22]. In this work we use this two-dimensional model to explore the effect of the mud consolidation process on the model results.

Even though good results were obtained with the 2D model regarding the hydrodynamic and fine sediment dynamics in the Río de la Plata, a three-dimensional approach allows to represent in more detail the sediment transport and stratification processes in this estuarine environment. The previous experience generated during the implementation of the 2D model paved the way for the three dimensional modules implementation. In this article we briefly describe the main characteristics of the modules set up and then present results from different sensitivity analysis with the circulation and sediment transport modules.

II. Study Area

The Río de la Plata is located on the east coast of South America. Its axis runs from NW to SE and is approximately 280 km long. Its surface area is approximately 35,000 km^2, and its width varies from 20 km at the innermost part to approximately 220 km at its mouth (Figure 1a). The river communicates freely with the ocean and experiences seasonal freshwater discharge from its two major tributaries (the Paraná and Uruguay rivers), with annual average discharge of approximately 16,000 m^3/s and 6,000 m^3/s, respectively. Two main regions can be identified based on the morphology and dynamics of the Río de la Plata. A shallow area located along the Punta Piedras-Montevideo line separates the inner region from the outer region. The inner region has a fluvial regime, with no stratification or preferential flow direction. In the outer region, the increase in river width generates complex flow patterns. This outer region is formed by brackish waters of

variable salinity that are influenced by the tides, the winds, and the contribution of fresh water from the river basin.

The tidal regime is dominated by the M2 component, followed by the O1 component which is responsible for the diurnal inequality. The tidal amplitude is greater along the Argentinean coast (order of 1 m), while it is about 0.4 m along the Uruguayan coast. The meteorological tide (storm surge events) is of great importance being of the same order of magnitude as the astronomical tide [23]. Currents at the estuary are controlled by the oceanic tide. Although the amplitude of the tides is small, the very large estuary mouth generates a tidal prism that can dominate the flow regime despite the significant discharge received from the tributaries.

The outer Río de la Plata and the adjacent continental shelf are covered with sands, while silty clays, clayey silts and silts, are confined to the upper and the middle portions of the estuary. The suspended sediment load is mainly carried by the Paraná river in amounts up to 160 million tons/year of fine sand, silt, and clay. Fine sands mostly settle in the innermost part of the Río de la Plata and are responsible for the Paraná Delta Front progradation [13]. Fluvial fine cohesive sediments are further advected to the inner part of the estuary.

Montevideo Bay covers an area of approximately 12 km^2 and is part of the Río de la Plata (Figure 1c). The water depth reaches 5 m in the outer part of the bay and between 1 m and 1.5 m in the inner area. The navigation channels are approximately 11 m deep. The bay receives two urban streams, Pantanoso and Miguelete. Water circulation in the bay mainly occurs due to the sea level variations along the bay mouth and due to shear induced by the outer flow and the local winds.

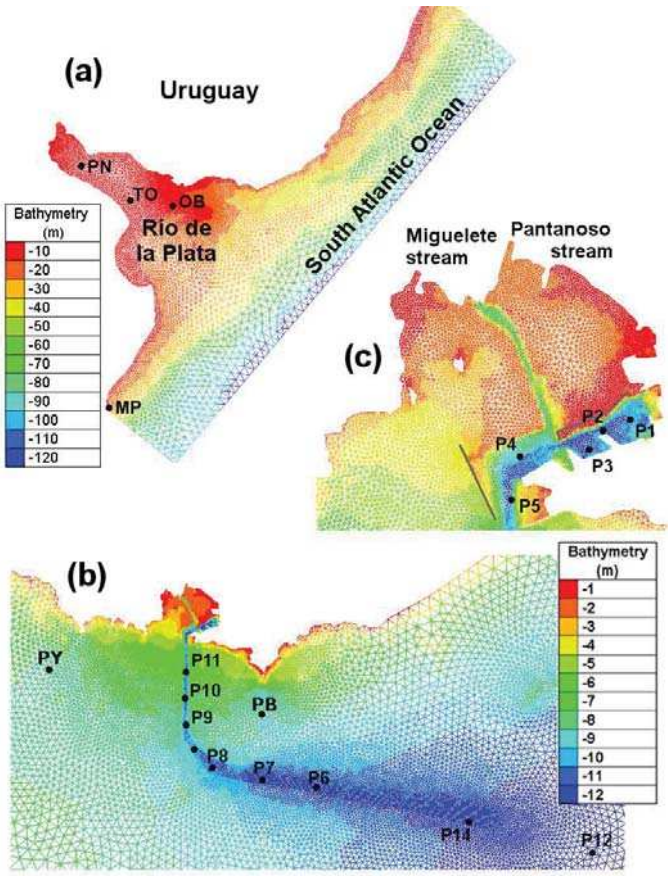

Fig. 1: (a) Río de la Plata unstructured mesh, (b) detail of Montevideo coastal area, (c) Montevideo Bay detail.

III. 2D HYDRODYNAMIC AND SEDIMENT TRANSPORT MODELLING: INFLUENCE OF THE CONSOLIDATION PROCESS

A consolidation model was chosen among the available options in the sediment transport model. The model was calibrated against settling column experiment results. A set of simulations was performed in order to initialize the bed and explore the impact of different erosion parameters configurations on the results. Finally a two years simulation including the consolidation process was performed and the results are compared against the ones obtained without considering this process.

A. *Consolidation multilayer algorithm*

Three different consolidation models are implemented in SISYPHE [26] [29]: multi-layer empirical algorithm, multi-layer iso-pycnal Gibson's model and vertical grid Gibson's model. We decided to use the second one as it has more physical meaning than the first one, and is less expensive from the computational point of view and more stable than the third one [29].

The consolidating muddy bed is discretized in layers of increasing concentrations, these concentrations being constant and imposed by the user. The determination of mass fluxes between consecutive layers is based on the Gibson's theory. This 1DV sedimentation-consolidation "multi-layer" model is based on an original technique to solve the Gibson equation, developed in [27]. Like in the previous model the concentration of different layers are fixed, the associated thicknesses are directly linked to the amount of sediment that they contain. The mass balance in layer i is:

$$\frac{M_i(t+\Delta t) - M_i(t)}{\Delta t} = F_i(t) - F_{i+1}(t) \tag{1}$$

where M_i is the mass of sediment in layer i, Δt the model time step, and F_i the sediment flux from the layer i to layer $i+1$.

As the model assumes the concentration of each layer to be constant over time, only the masses and thicknesses of these layers vary. The mass balance can be written in terms of the thicknesses of layers $Ep_i(t)$ (Figure 2) as follows:

$$Ep_i(t+\Delta t) = Ep_i(t) + \frac{(F_i(t) - F_{i-1}(t))\,\Delta t}{C_i} \tag{2}$$

As explained in [27] the sediment flux $F_i(t)$ can be written as:

$$F_i(t) = \frac{(V_{s,i}(t) - V_{s,i-1}(t))C_{i-1}C_i}{C_{i-1} - C_i} \tag{3}$$

where $V_{s,i}$ is the falling velocity of the layer i, defined as:

$$V_{s,i}(C_i) = \begin{cases} k(C_i)C_i\left(\frac{1}{\rho_s} - \frac{1}{\rho_f}\right), & if \quad C_i \leq C_{gel} \\ k(C_i)C_i\left(\frac{1}{\rho_s} - \frac{1}{\rho_f}\right) & \\ +k(C_i)\frac{\sigma'(C_{i-1}) - \sigma'(C_i)}{\frac{1}{2}(Ep_{i-1}(t) + Ep_i(t))}, & \text{otherwise} \end{cases} \tag{4}$$

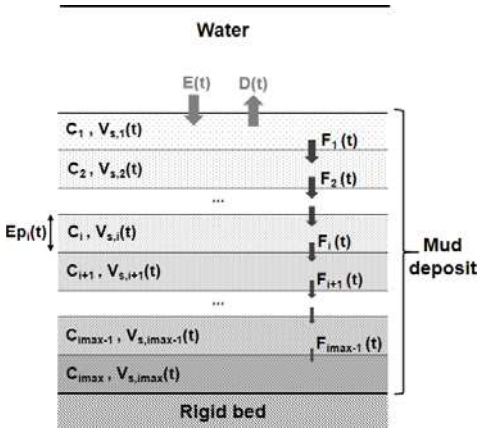

Fig. 2: Schematic vertical view of multilayer bed.

where ρ_s is the sediment density, k is the permeability, σ' is the effective stress, and C_{gel} the transition concentration between sedimentation and consolidation schemes [2]. There is not a standard methodology in the literature to determine the empirical functions for both permeability and effective stress, some alternatives are mentioned in this section.

For the determination of the closure equations for permeability and effective stress, most of study reported some fitting exercise on settling curve, i.e. the position of supernatant/suspension interface. They considered mostly the least square technique for the adjustment to experimental results. In this study we modified the module SISYPHE (subroutine `TASSEMENT_2.f`) in order to include the following closure equations as proposed in [27] and [28] :

$$k = \begin{cases} K_1 \left(\frac{C_i}{\rho_s} - 1\right)^{K_2}, & if \quad C_i \leq C_0 \\ K_3 \left(\frac{C_i}{\rho_s} - 1\right)^{K_4}, & if \quad C_i > C_0 \end{cases} \tag{5}$$

$$\sigma' = B_1 \left(B_2 - \frac{\rho_s}{C_i}\right)^{B_3} \quad if \quad C_i > C_0 \tag{6}$$

where K_1,K_2,K_3,K_4 and B_1,B_2,B_3 are constants to be determined during the calibration procedure.

B. Consolidation model calibration

The coefficients K_i and B_i in the closure equations for the permeability and effective stress (5 and 6) were determined by try and error comparing visually the experimental settling curve obtained in laboratory experiments. Several settling column experiments were carried out at the IMFIA (during FREPLATA-IFREMER Project founded by the French Fund for the Global Environment) using sediment samples from different zones of the estuary [4]. This simple laboratory 1D vertical (1DV) test is usually used to analyse the sedimentation and self-weight consolidation characteristics under motionless conditions [14], [24], [20]. The tests were focused on the influence of mud composition, initial concentration and salinity on the self-weight consolidation process. The experimental facilities consist of three 2 m height and 0.088 m diameter Plexiglas columns with measuring tapes in order to manually record the interfaces evolution. Each column was filled with a mixture of cohesive sediment and water and then the clear-muddy water interface and the bed-muddy water interface positions were registered over an extended time period. The main results were in good agreement with results available in the literature [14], [20].

In a later project [17] additional settling column experiments were made using mud samples taken in the Montevideo Bay area. Five settling column experiments were performed, considering different experiments durations and initial heights. At the end of some of these experiments the mud density was determined at three locations of the mud deposit. These locations are not precisely specified and were defined as "top of the deposit", "middle of the deposit" and "bottom of the deposit". In order to calibrate the closure equations for the permeability and effective stress we utilized the longest experiment. The mud used for this experiment had the following sediment size composition: 8% colloids, 39% clay, 52% silt and 1% fine sand. The initial concentration of the mixture of cohesive sediment and water was 93.2g/l, the initial mixture height was 0.987m and the experiment last 101 days. Unfortunately no density measurements were made at the end of this experiment, however we compare the model results against density measurements at the end of two shorter experiments (7 and 22 days duration).

In order to reproduce the settling column experiments a square domain of 1m x 1m with elements of 0.35m size was constructed, this does not has an effect on the results as we are looking at a 1DV process. The time step is 60 seconds and the simulations length 365 days. The bed was discretized using 20 layers with the following concentrations (g/l) from top to bottom: 100.; 120.; 140.; 160.; 180.; 200.; 220.; 240.; 260.; 280.; 300.; 325.; 350.; 375.; 400; 425.; 450.; 475.; 500.; 550.

The coefficients K_i and B_i were determined by try and error taking as reference values the ones presented by [27], the model showed to be very sensitive to all the parameters. Satisfactory results were obtained choosing the following values:

K_1=235 ; K_2=3.3 ; K_3=50 ; K_4=8 and C_0=150g/l

B_1=2.2.10^{-8} kg/m/s2 ; B_2=27 ; B_3=7.9

Figure 3 shows a comparison of the observed and simulated water-mud interface evolution for the longest experiment, the model is able to reproduce satisfactorily the experimental results. Figure 4 shows a comparison of concentrations values measured at the end of the shorter experiments, and the vertical concentration profiles obtained with the model at the same times. The measured concentration values have been located in approximate vertical positions representative of the "top of the deposit", "middle of the deposit" and "bottom of the deposit". As it can be seen the model give acceptable results when compared against observed concentration values.

C. Influence on the sediment transport and bed evolution

1) Bed initialisation and sensitivity to erosion parameters: A set of simulations was performed with two objectives: to initialize the bed and to explore different erosion parameters configurations. The bed is discretized using 20 layers with the concentration already presented in the consolidation model calibration. It is initialized with an initial thickness of 0.10m for layers 1 to 19, and 0.20m for layer 20 over the whole

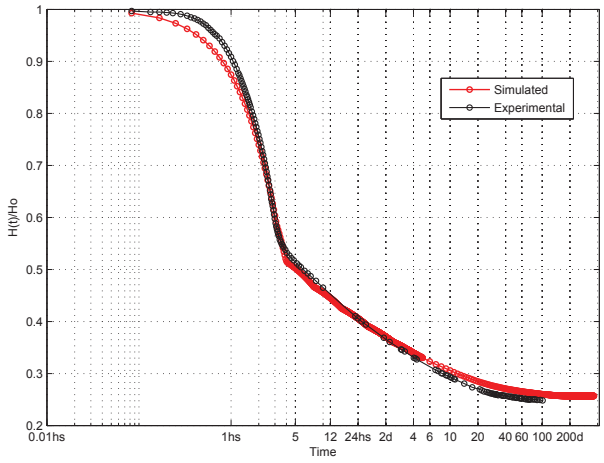

Fig. 3: Comparison of simulated and observed water-deposit interface evolution in the settling column experiment.

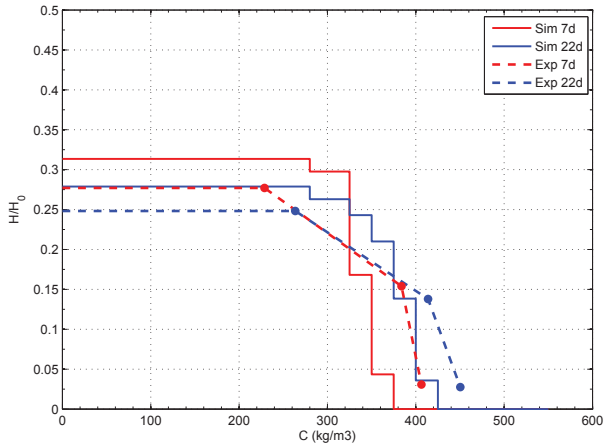

Fig. 4: Comparison of simulated vertical concentration profiles at 7 days (red) and 22 days (blue), against measured concentration values (dots with respective colours).

domain . Starting from this initial condition the period January 2009 to August 2010 (20 months) was simulated using realistic forcings. The consolidation of the initial bed generates a significant drop in the total bed height. In order to avoid modifications in the hydrodynamics due to this unrealistic drop of the bottom, the "STATIONARY MODE" keyword available in SISYPHE was utilized. That means TELEMAC2D does not receive any bottom elevation update during the simulation.

Three simulations were made increasing the complexity of the model in terms of the erosion parameters configuration. In the first simulation all the layers have the same parameter values (critical shear stress for erosion τ_{ce} and Partheniades coefficient M). The second one has different critical shear stress for erosion for each layer. The third one has both different critical shear stress for erosion and Partheniades constant for each layer.

The erosion parameters (τ_{ce} and M) relationship with the sediment concentration depends on the sediment and environment characteristics. Without any specific information for the Río de la Plata, and in order to explore the sensitivity of the model to these parametrisations, reasonable formulations presented in the bibliography from other study cases were used

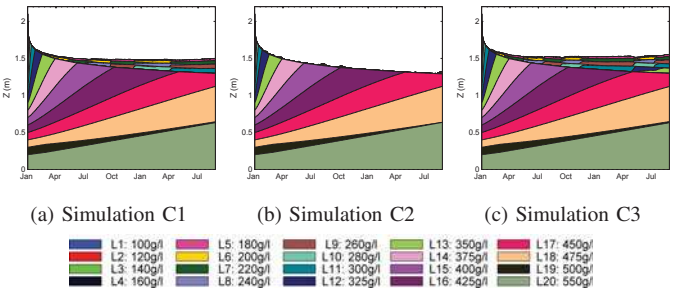

(a) Simulation C1 (b) Simulation C2 (c) Simulation C3

Fig. 5: Simulated temporal evolution of vertical bed concentration profile at Punta Brava during January 2009 - September 2010.

for this analysis. The constants in these formulations were modified in order to obtain critical shear stress for erosion of layer and Partheniades parameter values similar to those obtained during the sediment transport model calibration without the consolidation process [22] for concentrations around 350 g/l.

The parameters employed in simulation C1 are the ones which have been selected during the calibration of SISYPHE without consolidation. Then for the simulations C2 and C3 the critical shear stress depends on the layer concentration as follows:

$$\tau_{ce}^{i} = 10^{-6} C_i^2 \tag{7}$$

where C_i is the layer i concentration (kg/m^3), and $\tau_{c,e}^{i}$ the critical shear stress for erosion of layer i (Pa). This potential relationship between the critical shear stress for erosion and the concentration has been widely used with the exponent varying between 0.9 and 2.5 [12], [31].

For simulation C3 the selected relation between the Partheniades parameter and the layer concentration is [21]:

$$M^{i} = 10^{-13} C_i^3 \tag{8}$$

It is remarked again that the relationships among the erosion parameters and bed characteristics are strongly site-specific. Here reference relationships from biblography were considered in order to explore the effect of the consolidation process on the model results.

Figure 5 shows the temporal evolution of the vertical concentration profile at PB station (see Figure 1b) during the twenty simulated months for simulations C1, C2 and C3. Each layer, and its concentration, is identifiable by its colour. In all the simulations it is clearly appreciable the evolution of the initial bed sediment, which at the end of the simulation reaches a concentration of 450 g/l (L17) on its top layer and shows a decrease in its total height of approximately 0.7 m. Simulations C1 and C2 results show a "new" deposit of sediment over the initial one. The lower concentration of this deposit is close to 180 g/l while at the end of the 20 simulated months its maximum concentration reaches 300 - 350 g/l. On the other hand simulation C2 results do not show this new deposit, only few short episodes with net deposition are identifiable but the fresh deposit is quickly eroded.

Figure 6 shows examples of the SSC at several stations (see Figure 1) during 2009 and 2010. It is worth noting that in terms of the suspended sediment dynamics simulation C1

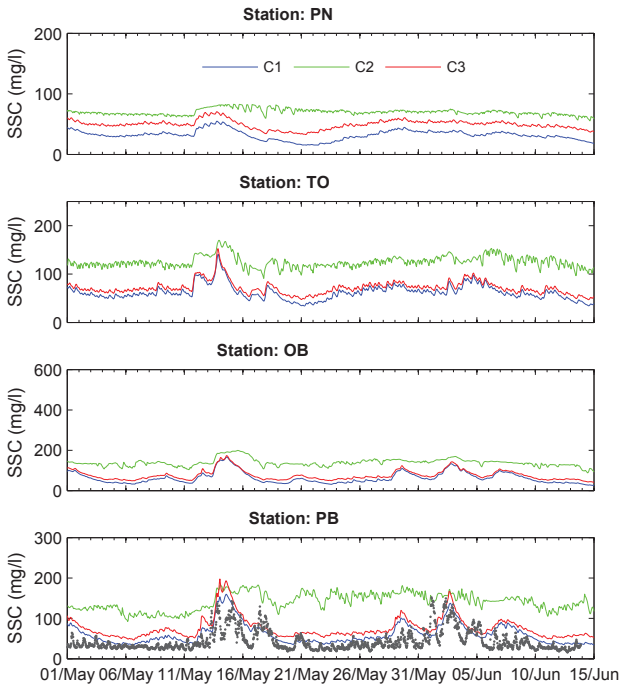

Fig. 6: SSC time series during May-June 2009 obtained with the different consolidation simulations.

produce the same results as the simulation without consolidation. Simulation C2 results shows that a lot of sediment is eroded and remains in suspension quasi permanently. This behaviour is coherent with the low value of critical shear stress for erosion of the low concentration layers. Because of that, in general the net flux is erosive in most of the estuary. Simulation C3 results show slightly higher values of SSC compared to simulation C1 results, but a very similar behaviour. In most of the estuary the top layer shows a concentration of 160 - 180 mg/l, the erosion parameters are much smaller than those obtained in the calibration without consolidation.

Based on this results it was decided to select the configuration of simulation C3 to make a longer simulation, not affected by the initial conditions of the bed, and see the impact on the bed evolution results.

2) Effect on the bottom evolution: Taking as initial condition the bed obtained at the end of simulation C3, it was made a two years long simulation using realistic forcings (2009-2010). The sediment transport model set up is the same utilized in simulation C3.

Figure 7 shows the bottom evolution during the second year of simulation with and without considering the consolidation process. In general terms there is not a significant change in the patterns of erosion and deposition zones. Lower values of accretion are obtained considering the consolidation process. In the inner-intermediate zone of the estuary areas where few changes in the bed elevation are observed without considering the consolidation process, then show a small decrease in the bed elevation.

As part of a project to study the nautical depth in the Montevideo Bay area [17], vertical bed density profiles in the navigation channels were measured using an instrument

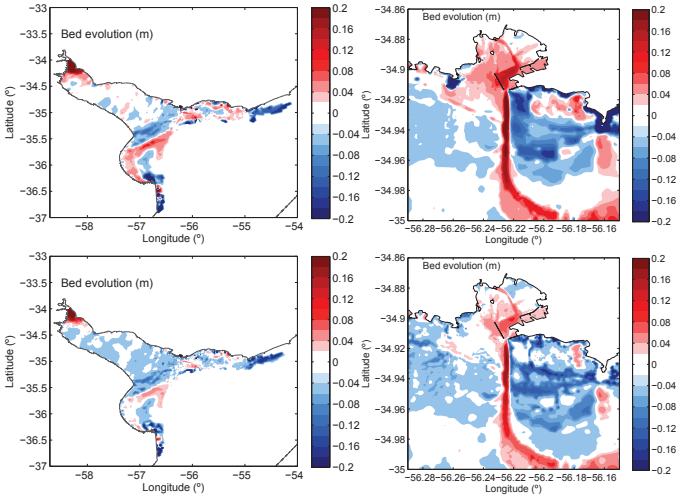

Fig. 7: Bottom evolution during the second year of simulation (2010) without consolidation (upper pannel) and considering it (lower pannel).

based on the tuning fork technology [7]. Figure 8 shows a comparison between the simulated and measured vertical mud concentration profiles at several points inside the bay and along the navigation channel (see Figure 1b,c). In general there is a very good agreement between the model results and the measurements. Stations P1 to P4 are located in the harbour area inside the bay, the model represents well the concentration in the upper layer as well as the profile shape, and slightly overestimates the higher concentration values for depths greater than 0,5 m approximately. In the stations located on the access channel the model results reasonable good. In the outter stations (P12 to P14) located at the beginning of the access channel the model is able to reproduce a higher increase of the mud concentration with the depth inside the bed.

IV. 3D HYDRODYNAMIC AND SEDIMENT TRANSPORT MODELLING

A. Domain and computational mesh

The modelled domain and horizontal mesh are the same that were utilized for the 2D model. It includes the Rio de la Plata and its maritime front zone approximately until the 200 m depth on the continental shelf (Figure 1a). The main freshwater inflows are included, rivers Paraná and Uruguay at the north-west boundary. The mesh elements size ranges from approximately twelve kilometres at the oceanic boundary to ten meters in the vicinity of the Montevideo Bay, it has 30059 nodes and 58594 elements. Figure 1b and c show the mesh at Montevideo Bay zone and includes its bathymetry. It can be seen the navigation channel which gives access to Montevideo's harbour and the harbour basins and internal channels in the bay.

1) Circulation module: The hydrodynamic module TELEMAC 3D was implemented for the selected domain taking into account the fluvial discharges of Paraná and Uruguay rivers, tides at the oceanic boundary (astronomical and meteorological from a regional model), and wind and sea level pressure from ERA-Interim ReAnalysis. The subroutines `BORD3D.f` and `METEO.f` were modified in order to impose oceanic and meteorological boundary conditions with

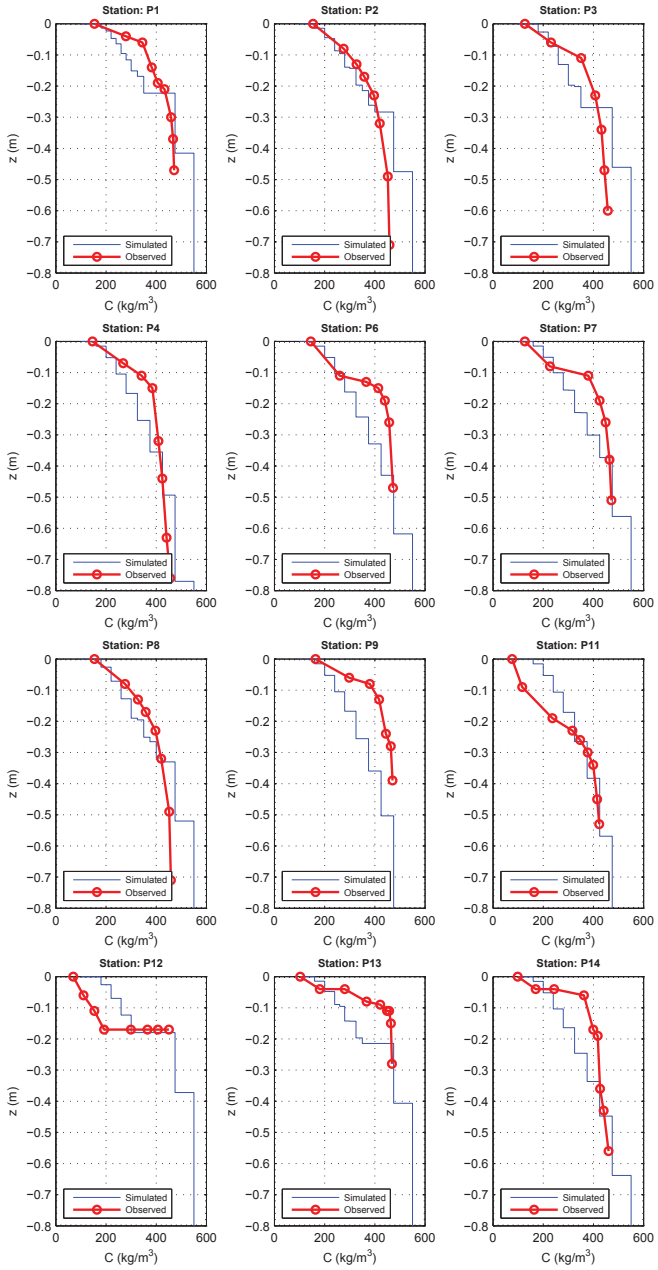

Fig. 8: Comparison of observed vertical mud density profiles and simulation results at the end of a two years simulation.

temporal and spatial variability. The daily flow information of the Paraná and Uruguay rivers was provided by the Argentinian National Water Institute. Relevant tidal waves, both astronomical and meteorological, are imposed at the oceanic open boundary. Sea surface elevation values provided by a regional tidal model [11] are prescribed at oceanic boundary nodes. On the free surface, wind and sea level pressure forcings are considered. For the wind surface stress ($\overrightarrow{\tau}_{wind}$) an aerodynamic bulk formula is employed (9). The wind drag coefficient was selected as a calibration parameter.

$$\overrightarrow{\tau}_{wind} = \frac{\rho_{air}}{\rho_{water}} a_w \mathbf{U_w} \|\mathbf{U_w}\| = C_d \mathbf{U_w} \|\mathbf{U_w}\| \qquad (9)$$

where C_d is the wind drag coefficient, $\mathbf{U_w} = (U_w, V_w)$ the components along the x and y directions of wind veolcity 10m above the water, and ρ_{water} and ρ_{air} the water and air densities respectively. The wind drag coefficient can be set as constant value or as a function of the wind velocity using the formulation proposed by [3]:

$$a_w = \begin{cases} 0.565 \times 10^{-3} & \text{if} \quad \|\mathbf{U_w}\| \leq 5\text{m/s} \\ (-0.12 + 0.137\|\mathbf{U_w}\|) \times 10^{-3} & \\ \text{if} \quad 5\text{m/s} \leq \|\mathbf{U_w}\| \leq 19.22\text{m/s} & \\ 2.513 \times 10^{-3} & \text{if} \quad \|\mathbf{U_w}\| \geq 19.22\text{m/s} \end{cases} \qquad (10)$$

where $\|\mathbf{U_w}\|$ is the wind velocity module.

Both the salinity and suspended fine sediment were considered in the simulations and modelled as active tracers. The turbulence is modelled using the $k-\varepsilon$ model.

Regarding the bottom friction computation, several tests were performed using the Nikuradse formulation for turbulent rough bed conditions [18] and the Reichardt equation for hydraulically smooth conditions [19]. For this study case the results showed a small impact of the bottom roughness on the hydrodynamic variables, SSE and currents. The sensitivity analyses presented here were made using the Nikuradse bottom friction formulation for hydraulically rough conditions with k_s=0.1mm.

2) Wave module: The third generation spectral wave model TOMAWAC is forced with 10m wind from the European Centre of Medium Weather Forecast ERA-Interim Reanalysis. At the oceanic boundary the model is forced by wave statistics from a regional model [1]. A Jonswap spectrum is constructed at each boundary node based on the significant wave height, peak period, mean direction, and directional spread given by the regional model with a temporal resolution of 3 hours. The model was configured to takes into account the following processes: white capping, bottom friction, depth breaking, and quadruplets interactions.

3) Sediment transport module: As well as for the bi-dimensional model only one sediment class is considered, which is defined as cohesive. The bed is assumed to be uniform over the domain, however areas where non-cohesive sediments are predominant were set as non-erodables. In order to compute the erosion and deposition fluxes the classical Krone and Partheniades laws were applied [9], [16]. The parameters to be defined are the settling velocity, the Partheniades coefficient, and both the critical shear stress for deposition and erosion. The consolidation process was not taken into account in the three-dimensional model.

The set of subroutines dealing with sediment transport processes in TELEMAC3D, called SEDI3D [10], treats the settling velocity as a constant value, however it is greatly influenced by the flocculation process. The major factors that control this process are the suspended sediment concentration (SSC), the turbulence and the shear stress [32]. In this study the code was modified (subroutine `VITCHU.f`) in order to make the settling velocity dependent on the SSC based on the following relationship [5], [6], [15], [30]:

$$W_s = W_s^0 \left(\frac{C}{C_0} \right)^m \qquad (11)$$

being C the suspended sediment concentration, W_s^0 a reference settling velocity corresponding to the depth-averaged suspended sediment concentration C_0, and m is a coefficient

between 0.5 and 3.5 [30]. Without any experimental estimation for the Río de la Plata, after testing different values for the coefficient m it is taken to be equal 1.

The boundary and initial conditions are as well the same utilized for the 2D model. The SSC imposed at the boundaries is zero except for the two sections corresponding to Uruguay and Paraná Rivers. At Paraná Las Palmas boundary the imposed SSC is 47 mg/L, while at Uruguay and Paraná Guazú boundary it is 154 mg/L.

For the sensitivity analysis the initial condition was a null value of SSC for the whole domain. At the erodable area the bed is composed of cohesive sediment with a concentration of 450 g/l, there is no limitation on the available sediment to be eroded.

4) Coupled Circulation, Wave and Sediment transport: The three dimensional module TELEMAC 3D, including the sediment transport library SEDI3D can be run internally coupled with the wave module TOMAWAC. The exchange information among the different modules take place at a user defined coupling period. The circulation module TELEMAC 3D is the leading code and calls TOMAWAC. Only depth averaged information is exchanged between the circulation and wave modules.

As the wave module increases the computation time considerably, in the same way it was made for the bi-dimensional model [22] an alternative coupling procedure is proposed in order to save computational time. In this case it was decided to use the wave model results obtained with previous simulations of the 2D morphodynamic model TELEMAC2D-TOMAWAC-SISYPE. The corresponding subroutines of SEDI3D (`CLSEDI.f`) were modified in order to read the wave parameters from the results file of these previous simulations. The wave induced bottom shear stress, which is essential for the sediment transport library, was computed using the Swart formulation [25] based on the significant wave hegiht and peak period provided by TOMAWAC and using a Nikuradse equivalent bottom roughnes k_s=0.1mm.

The total bottom shear stress is computed by a vectorial addition between the currents and waves bottom stress, considering the currents direction and the mean wave propagation direction.

$$\tau_{cw} = \sqrt{\tau_c^2 + 2\tau_c\tau_w \left|\cos\varphi\right| + \tau_w^2} \qquad (12)$$

where τ_c is the currents induced bottom shear stress, τ_w is the wave induced bottom shear stress, and φ the angle between the currents direction and the mean wave propagation direction.

B. Sensitivity analysis

In this section it is analysed the sensitivity of the model results to the wind drag coefficient, and also to the sediment transport model parameters. The later is divided in two based on the sediment exchange paradigm, exclusive versus simultaneous erosion-deposition paradigms [8]. These two approaches are very different, and so it is the behaviour of the model results. For each paradigm it is analysed the sensitivity to the settling velocity (W_s), the Partheniades coefficient (M), and both the critical shear stress for deposition and erosion (τ_{cd}, τ_{ce}).

It was performed a sensitivity analysis to the number of vertical layers (not shown here), in which we used 10, 16, 20, 30 sigma levels equally spaced along the vertical. Even though increasing the number of vertical layers provides a higher vertical resolution, the simulations became more expensive form a computational point of view. For example, if we take as a reference the computation time required to complete the simulation with 9 layers, then the computation time taken by the simulation with 15 layers was approximately 20% higher, the simulation with 20 layers approximately 55% higher and with 30 layers 360% higher. From the sensitivity analysis we conclude that the number of vertical layers does not have an appreciable effect on the sea surface elevation behaviour. Minor differences can be observed in the currents and salinity results. Using more than 16 layers gave very similar results. Taken into account this it was decide to use 16 sigma levels.

1) Wind drag coefficient influence: Five simulations were made in order to evaluate the influence of the wind drag coefficient on the model results. The considered C_d values are presented in Tabel I, the first simulation is called "Ref" as it is the reference value utilized in the bi-dimensional model. For the last simulation (CD4) the wind drag coefficient is computed using the formulation presented in (10).

TABLE I: Sensitivity simulations to the wind drag coefficient.

Simulation	Ref	CD1	CD2	CD3	CD4
C_d	3×10^{-6}	2×10^{-6}	4×10^{-6}	5×10^{-6}	Variable

Figure 9 shows the sea surface elevation series at the station MP, PB and PN during August 2010. As it can be seen the wind drag coefficient has an appreciable influence on the results specially during storm surge events (e.g. 14th August). There are differences between the SSE obtained with simulations CD1 and CD3 (lowest and highest C_d respectively) which exceed 1m.

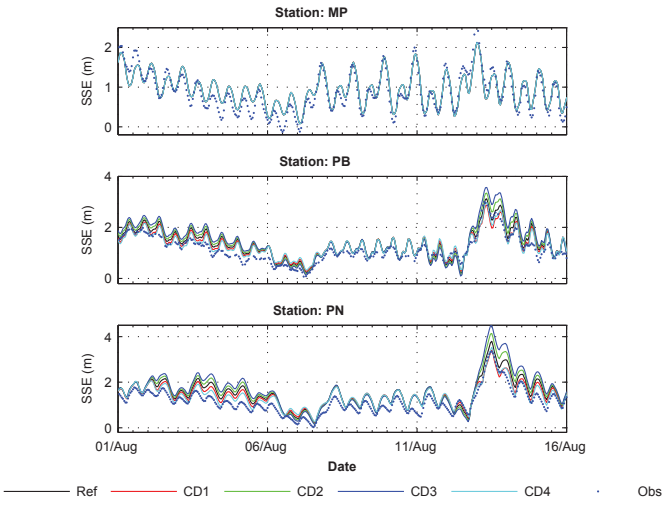

Fig. 9: SSE elevation series during August 2010.

Figure 10 shows a comparison among the measured and simulated current intensity and direction at the station OB. Three bins are shown, being the bin 2 the closest to the bottom. The model results where vertically interpolated to the estimated bin height of the ADCP. The influence of the wind drag coefficient is noticeable both on the currents intensity and directions.

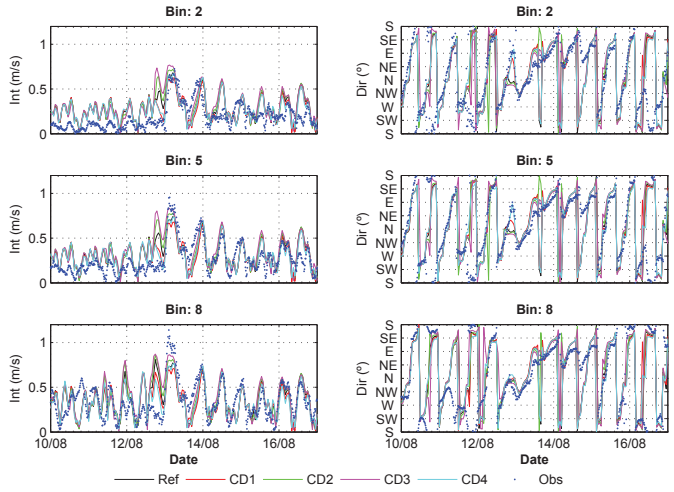

Fig. 10: Currents series at OB during August 2010.

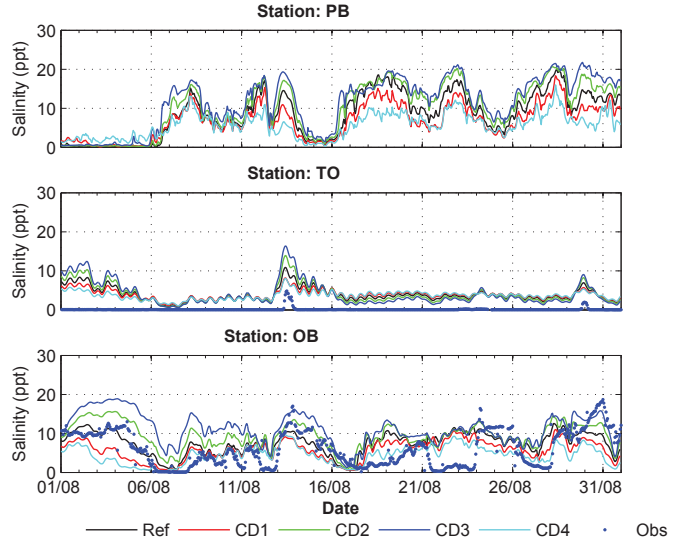

Fig. 11: Salinity series at PB, TO and OB during August 2010.

Figure 11 shows the salinity time series at the station PB, TO and OB during August 2010 obtained with the different model configurations in the mid water column (layer 5). At the last two stations observed data were also included. The influence of the wind drag coefficient on the salinity field is important. The model results shows the ability of the model to capture the main characteristics of the salinity front mobility.

2) Erosion-deposition paradigms:

a) Exclusive erosion-deposition paradigm: Table III shows the parameters for the nine simulations performed using this erosion-deposition paradigm. In order to facilitate the comparison of the results among the different simulations are grouped first taking into account the value of the Partheniades coefficient (M), three values were tested: 3×10^{-7}, 1×10^{-6} and 3×10^{-6} kg/m^2/s. Then for each of these values different critical shear stress for deposition and erosion (τ_{cd}, τ_{ce}) were tested: 0.10, 0.15 and 0.20 Pa. Finally for the last subset of simulations also different values of W_s^0 were considered (being the reference concentration C_0 in (11) equal to 0.1g/l).

Figure 12 shows the SSC series at the bottom and surface layers at the stations PN,PB, TO and OB during August 2010.

TABLE II: Exclusive erosion-depostion (EED) simulation set parameters.

	$W_s^0(mm/s)$	$\tau_{ce}(Pa)$	$\tau_{cd}(Pa)$	$M(kg/m^2/s)$
EED 1	0.1	0.20	0.20	3×10^{-7}
EED 2	0.1	0.10	0.10	3×10^{-7}
EED 3	0.1	0.20	0.20	1×10^{-6}
EED 4	0.1	0.15	0.15	1×10^{-6}
EED 5	0.1	0.10	0.10	1×10^{-6}
EED 6	0.1	0.20	0.20	3×10^{-6}
EED 7	0.1	0.15	0.15	3×10^{-6}
EED 8	0.5	0.20	0.20	3×10^{-6}
EED 9	0.02	0.20	0.20	3×10^{-6}

As it can be seen the effect of the Partheniades coefficient M on the results is very strong. By comparing for example the simulations EED1, EED3 and EED6 we can see that increasing M increase the base SSC value and also magnitude of the storm resuspension event. It has a dramatic impact on the maximum SSC values at the bottom layer during the storm events, note that for the higher values of M SSC up to near 200g/l are reached at PB station. As expected the effect of critical shear stress for deposition and erosion (τ_{cd}, τ_{ce}) is also important, decreasing the threshold value increases the base SSC values and of course the magnitude of the storm resuspension events.

In the last subset of simulations two simulations with different settling velocities were included. As it can be seen in Figure 12 with $W_s^0 = 0.1$mm/s after the storm resuspension events it takes several days to return to the base SSC values. If we decrease the W_s^0 value the sediment remains in suspension for a longer time, increasing the base SSC values associated to the tidal forcing and also extending the time required to go back to normal conditions after the storm events. As it can be seen if we use $W_s^0 = 0.1$mm/s it takes weeks for the SSC to decrease after the storm events. On the other hand, increasing W_s^0 up to 0.5 mm/s effectively decreases the time required to go back to normal conditions after the storm events, but also strongly decrease the base SSC values. If we look at the impact on the bottom SSC values, higher settling velocity values leads to higher bottom SSC values and vice versa. On one hand a higher settling velocity value implies that the sediment will settle faster so it is expected to have higher bottom SSC values, on the other hand it also implies that the deposition flux will be higher which tends to decrease the bottom the SSC values. As observed in 12 it seems that the first effect prevails, so decreasing the settling velocity increase the base SSC values and decrease the maximum bottom SSC values.

Figure 13 shows the bottom evolution during the period July-August 2010 at the station P10 (see Figure 1b) located in the S-N section of the access channel to the Montevideo Bay, and the value of the maximum SSC during the simulated period. Based on the dredging activities a rough estimation of the siltation rates in the navigation channel at station P10 is between 0.20-0.30 m after two months. Increasing M increases the siltation rate at the navigation channel, however it also increases the maximum SSC value up to concentration far too high. It is interesting to note the effect of the settling velocity on the navigation channel siltation rate. Comparing simulations EED6, EED8 and EED9 we can see that even though the lowest settling velocity (EED9) shows higher base SSC values

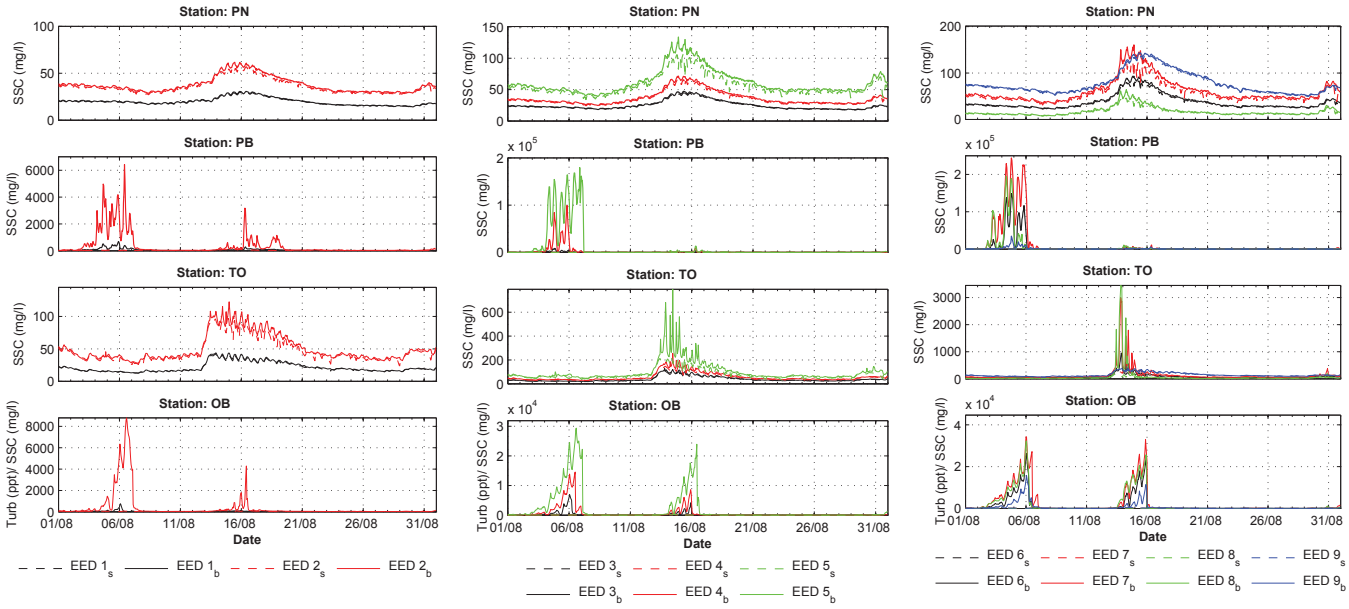

Fig. 12: Bottom and surface SSC series during August 2010 for the EED paradigm simulations.

the siltation rate is lower. A higher value of settling velocity leads to higher SSC near the bottom and higher deposition flux inside the navigation channel. Furthermore it can be seen that the high siltation rates obtained for simulations EED 5 to EED 8 take place due to very high concentrated sediment suspensions moving near the bottom which are captured by the navigation channel due to its geometry and favourable conditions for sediment deposition.

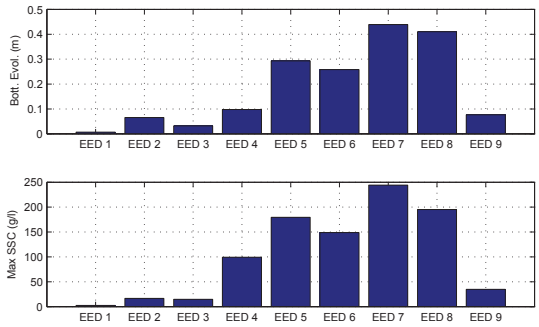

Fig. 13: Bottom evolution at station P10 and maximum SSC during the period July-August 2010 for the EED paradigm simulations.

In summary, the influence of M on the SSC results is very important, and depends on the selected τ_c. In many of these simulations the maximum bottom SSC are far to high, and actually out of the hypothesis of the model. Suspensions with concentrations higher than 80 g/l can be considered as low density fluid mud [12] and can not be modelled as a Newtonian fluid and so the model results are conceptually wrong. Even playing with the three parameters it is very difficult to find a set fulfilling the general characteristics of the suspended sediment dynamics in the whole estuary under this paradigm. The rate of SSC decreasing after the storm events showed to be mainly controlled by the W_s value. High values of settling velocity are needed in order to reproduce the observed behaviour after storm events, however this leads to lower values of SSC during calm conditions specially at the inner zone of the estuary. The way to increase the base SSC would be to decrease the critical shear stress for erosion or increase the Partheniades coefficient, however this will leads to higher maximum bottom SSC which are out of the hypothesis of the present model.

b) Simultaneous erosion-deposition paradigm: Table III shows the parameters utilized for the six simulations performed using the simultaneous erosion-deposition paradigm. In the first three simulations (SED 1 to SED 3) the Partheniades coefficient is increased leaving the other parameters unchanged, the tested values are: 3×10^{-6}, $1.\times10^{-5}$ and 3×10^{-5}. In the following simulations SED 4 the effect of increasing the reference settling velocity W_s^0 from 0.1 mm/s up to 0.5 mm/s is tested. Simulation SED 5 has a higher critical shear stress for erosion threshold (0.15 Pa) compared to simulation SED 4 (0.1Pa). Finally simulation SED 6 is not directly comparable to any of the previous simulations, it has the lowest settling velocity and a low Partheniades coefficient value.

TABLE III: Simultaneous erosion-depostion (SED) simulation set parameters.

	$W_s^0(mm/s)$	$\tau_{ce}(Pa)$	$M(kg/m^2/s)$
SED 1	0.1	0.10	3×10^{-6}
SED 2	0.1	0.10	1×10^{-5}
SED 3	0.1	0.10	3×10^{-5}
SED 4	0.5	0.10	3×10^{-5}
SED 5	0.5	0.15	3×10^{-5}
SED 6	0.05	0.10	5×10^{-6}

Figure 14 shows the SSC series at the bottom and surface layers at the stations PN, PB, TO and OB during August 2010. It can be seen that increasing the Partheniades coefficient increases the base SSC value, the SSC during the storm events and also amplifies a signal with semi diurnal frequency clearly related to the astronomical tide. Simulation SED 4 has a settling velocity five times higher compared to simulation SED 3. As it can be seen the effect is to decrease strongly the base SSC value and the maximum SSC during the storm events, the signal with tidal frequency is still clearly noticeable in station like PN and TO. Simulation SED 5 results are similar to those

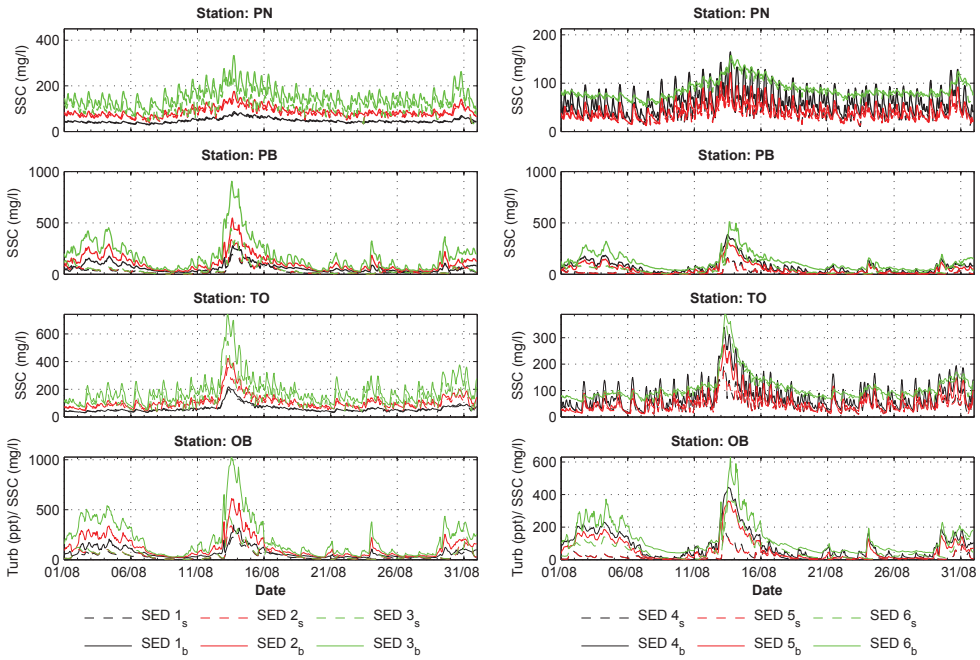

Fig. 14: Surface and bottom water SSC series during July-August 2010 for the SED paradigm simulations.

obtained with simulation SED 4, being the only difference between them an increase of the erosion threshold from 0.1Pa to 0.15 Pa. The differences are more noticeable at the inner stations, being as expected the SSC values slightly lower in the simulation SED 5. Finally about the simulation SED 6 results, it is first interesting to note their similitude to those obtained with the simulation SED 2. Moreover, the base SSC value is similar between them and also the maximum SSC during storm events, however the signal with tidal frequency is much smaller in simulation SED 6 results. Simulation SED 6 has a lower settling velocity and a lower Partheniades coefficient, both approximately half of the values utilized in simulation SED 2.

Figure 15 shows the bottom evolution during the period July-August 2010 at the station P10, and the value of the maximum SSC during the simulated period. In the first three simulations, increasing M increases the siltation rate the navigation channel as well as it also increases the maximum SSC value. In this case the maximum SSC values are still under the hypothesis of the present model.

The effect of the settling velocity on the navigation channel siltation rate is the opposite to the one obtained with the EED paradigm. As we can see comparing simulations SED 3 and SED 4 results, a higher settling velocity (SED 4) shows both lower SSC values and siltation rate in the navigation channel. Under this paradigm deposition occurs continuously, a higher settling velocity leads to lower SSC near the bottom. Taking into account the settling velocity formulation presented in 11, the deposition flux has the following expression:

$$D = W_s \times C = \frac{W_s^0}{C_0} \times C^2 \qquad (13)$$

So even though increasing W_s^0 tends to increase D, the lower SSC values near the bottom have the opposite effect which seems to prevail.

Finally even though simulations SED 6 and SED 2 results have similar SSC values, the navigation channel siltation obtained with simulation SED 6 is lower. This is in fact reasonable taking into account the deposition flux expression (13), as similar SSC values are obtained in both simulations with a lower settling velocity value in simulation SED 6.

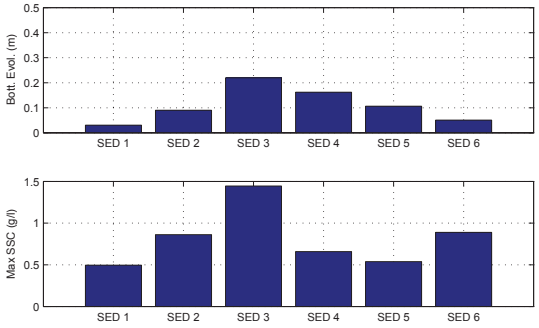

Fig. 15: Bottom evolution at station P10 and maximum SSC during the period July-August 2010 for the SED paradigm simulations.

V. Discussion and Conclusion

The influence of the consolidation process on the sediment transport module was explored modifying a multi-layer isopycnal Gibson's model available in SISYPHE. The closure equations for the permeability and effective stress were calibrated based on settling column experiments, the model results were very sensitive to the calibration parameters. Good agreement was found between measured vertical density profiles and the model results. Including the consolidation model allowed us to have spatial variability on the erosion parameters. In zones where erosion is dominant the top layer, exposed to the hydrodynamic action, has higher sediment concentration and so a higher critical shear stress for erosion. The simulated suspended sediment dynamics behaviour in the Montevideo

Bay area does not show significant differences compared to the results without consolidation. A possible explanation is that in contrast with other estuaries, at the Río de la Plata only a few centimetres of the bed are eroded (maximum SSC in general do not exceed 1g/l) even during the storm events. So in our simulations with the 2D model the bed-water column sediment exchange usually is not enough to involve more than one layer of the bed.

A three dimensional hydrodynamic and sediment transport model was successfully implemented for the study area. A sensitivity analysis to the wind drag coefficient showed that it has a significant impact on the model results. It has a noticeable impact on the SSE specially during the storm surge events. The effect on the currents and salinity distribution is linked and also influenced by the vertical mixing. Higher C_d values leads to a location of the salinity front further inside the estuary and less vertical stratification. The results obtained with the variable wind drag coefficient are closer to those obtained with the lower C_d values.

We have evaluated the effect of the erosion-deposition parameters on the model results under two different erosion-deposition paradigms. As it was shown with the exclusive erosion-deposition paradigm high values of settling velocity are needed in order to reproduce observed SSC behaviour after the storm events. This leads to low base values for the SSC in calm conditions, which can be compensated by increasing the Partheniades coefficient or decreasing the critical shear stress for erosion threshold. All these actions tends to increase the bottom SSC, which already was far too high in all the tested configurations. This was in fact the main problem found with this paradigm, the maximum bottom SSC during storm events are out of the hypothesis of the present model. Increasing the critical shear stress threshold for deposition would help to decrease the high bottom SSC values, however it implies also increasing the critical shear stress for erosion which will not allows us to represent the base SSC values in calm conditions. So it was not possible to find a combination of parameters representing properly the general dynamics of the suspended sediment dynamics of the estuary keeping the SSC values under the range of applicability of the present model.

On the other hand with the simultaneous erosion-deposition paradigm it was much easier to find several set of parameters capturing some of the main characteristics of the fine sediment dynamics in the estuary. The Partheniades coefficient showed to have an interesting effect on the SSC signal related to the astronomical tide. As it was shown different combinations of parameters can give similar SSC results (SED 2 versus SED 6 simulations), having however different results on the navigation channel siltation. The effect of the settling velocity on the navigation channel siltation rate is the opposite to the one obtained with the EED paradigm, increasing the settling velocity leads to lower siltation rates.

Based on this sensitivity analysis the simultaneous erosion-deposition paradigm will be adopted for future works. The exclusive erosion-deposition paradigm seems to be an interesting option to consider if the model is extended to include a description of the fluid mud behaviour, as well as the consolidation process.

ACKNOWLEDGMENT

This work was conducted within the Uruguayan - French cooperation project ECOS-Sud U014U01.

REFERENCES

[1] R. Alonso, "Evaluación del potencial undimotriz de Uruguay," Master's thesis, Universidad de la República, Uruguay, Dec. 2012.

[2] B. Camenen and D. Pham van Bang, "Modelling the settling of suspended sediments for concentrations close to the gelling concentration," *Continental Shelf Research*, vol. 31, no. 10, pp. S106–S116, Jul. 2011. [Online]. Available: http://linkinghub.elsevier.com/retrieve/pii/S0278434310002219

[3] R. Flather, "Results from surge prediction model of the north-west european continental shelf for april, november and december 1973." Institute of Oceanography (UK), Report 24, 1976.

[4] M. Fossati and I. Piedra-Cueva, "Self-weight consolidation tests of the río de la plata sediments," in *INTERCOH 2015 13th International Conference on Cohesive Sediment Transport Processes: 7-11 September 2015 Leuven, Belgium : book of abstracts*. Flanders Marine Institute, 2015.

[5] G. Franz, L. Pinto, I. Ascione, M. Mateus, R. Fernandes, P. Leitão, and R. Neves, "Modelling of cohesive sediment dynamics in tidal estuarine systems: Case study of Tagus estuary, Portugal," *Estuarine, Coastal and Shelf Science*, vol. 151, pp. 34–44, Dec. 2014. [Online]. Available: http://www.sciencedirect.com/science/article/pii/S0272771414002698

[6] O. Gourgue, W. Baeyens, M. Chen, A. de Brauwere, B. de Brye, E. Deleersnijder, M. Elskens, and V. Legat, "A depth-averaged two-dimensional sediment transport model for environmental studies in the Scheldt Estuary and tidal river network," *Journal of Marine Systems*, vol. 128, pp. 27–39, Dec. 2013. [Online]. Available: http://linkinghub.elsevier.com/retrieve/pii/S0924796313000833

[7] V. Groposo, R. L. Mosquera, F. Pedocchi, S. B. Vinzón, and M. Gallo, "Mud Density Prospection Using a Tuning Fork," *Journal of Waterway, Port, Coastal, and Ocean Engineering*, vol. 141, no. 5, p. 04014047, 2015. [Online]. Available: http://ascelibrary.org/doi/10.1061/%28ASCE%29WW.1943-5460.0000289

[8] H. Ha and J.-Y. Maa, "Evaluation of two conflicting paradigms for cohesive sediment deposition," *Marine Geology*, vol. 265, no. 3-4, pp. 120–129, Sep. 2009. [Online]. Available: http://linkinghub.elsevier.com/retrieve/pii/S0025322709001765

[9] R. Krone, "Flume studies of the transport of sediment in estuarial shoaling processes." Hydraulic Engineering Laboratory and Sanitary Engineering Research Laboratory. University of California, Berkeley., Tech. Rep., 1962.

[10] C. LeNormant, "Description of sedi3d, the sediment library of telemac-3d release 2.2." EDF R$D LNHE, Tech. Rep., 2002.

[11] C. Martínez, J. Silva, E. Dufrechou, P. Santoro, M. Fossati, P. Ezzatti, and I. Piedra-Cueva, "Towards a 3d hydrodynamics numerical modeling system for long term simulations of the río de la plata," in *36th IAHR World Congress*, 2015.

[12] A. J. Mehta, *An introduction to hydraulics of fine sediment transport*, ser. Advanced series on ocean engineering. New Jersey: World Scientific, 2014, no. volume 38.

[13] A. Menéndez and A. Sarubbi, "A model to predict the paraná deltafront advancement," in *Workshop on Morphodynamic Processes inLarge Lowland Rivers*, 2007.

[14] C. Migniot, "Tassement et rhéologie des vases. Première partie," *La Houille Blanche*, no. 1, pp. 11–29, Feb. 1989. [Online]. Available: http://www.shf-lhb.org/10.1051/lhb/1989001

[15] J. Nicholson and B. A. O'Connor, "Cohesive Sediment Transport Model," *Journal of Hydraulic Engineering*, vol. 112, no. 7, pp. 621–640, Jul. 1986. [Online]. Available: http://ascelibrary.org/doi/10.1061/%28ASCE%290733-9429%281986%29112%3A7%28621%29

[16] E. Partheniades, "A study of erosion and deposition of cohesive soils in salt water." Ph.D. dissertation, University of California, Berkeley, 1962.

[17] F. Pedocchi, V. Groposo, R. Mosquera, and I. Piedra-Cueva, "Estudio de la profunidad náutica del puerto de montevideo." IMFIA - Facultad de Ingeniería - Universidad de la República, Report, 2012.

[18] S. B. Pope, *Turbulent flows*. Cambridge ; New York: Cambridge University Press, 2000.

[19] H. Reichardt, "Vollständige Darstellung der turbulenten Geschwindigkeitsverteilung in glatten Leitungen," *ZAMM - Zeitschrift für Angewandte Mathematik und Mechanik*, vol. 31, no. 7, pp. 208–219, 1951. [Online]. Available: http://doi.wiley.com/10.1002/zamm.19510310704

[20] H. Samadi-Boroujeni, M. Fathi-Moghaddam, M. Shafaie-Bajestan, and H. M. Vali-Samani, "Chapter 13 Modelling of sedimentation and self-weight consolidation of cohesive sediments," in *Proceedings in Marine Science*. Elsevier, 2008, vol. 9, pp. 165–191. [Online]. Available: http://linkinghub.elsevier.com/retrieve/pii/S1568269208800150

[21] L. P. Sanford and J. P.-Y. Maa, "A unified erosion formulation for fine sediments," *Marine Geology*, vol. 179, no. 1-2, pp. 9–23, 2001. [Online]. Available: http://linkinghub.elsevier.com/retrieve/pii/S0025322701002018

[22] P. Santoro, M. Fossati, P. Tassi, N. Huybrechts, D. Pham Van Bang, M. Benoit, and I. Piedra-Cueva, "Hydrodynamic and fine sediment transport numerical modelling, application to the río de la plata and montevideo bay," in *Proceedings of the XXIIth Telemac-Mascaret User Club*, 2015, pp. 119–126.

[23] P. E. Santoro, M. Fossati, and I. Piedra-Cueva, "Study of the meteorological tide in the río de la plata," *Continental Shelf Research*, vol. 60, pp. 51–63, 2013. [Online]. Available: http://linkinghub.elsevier.com/retrieve/pii/S0278434313001180

[24] G. C. Sills and K. Been, "Self-weight consolidation of soft soils: an experimental and theoretical study," *Géotechnique*, vol. 31, no. 4, pp. 519–535, Jan. 1981. [Online]. Available: http://www.icevirtuallibrary.com/content/article/10.1680/geot.1981.31.4.519

[25] D. Swart, *Offshore sediment transport and equilibrium beach profiles*, ser. Publications // Delft Hydraulics Laboratory. W.D. Meinema B.V., 1974. [Online]. Available: https://books.google.fr/books?id=qYYNAQAAIAAJ

[26] P. Tassi and C. Villaret, *Sisyphe v6.3 User's Manual*, 1st ed., EDF R&D, 6 quai Watier - 78401 CHATOU, 1 2014.

[27] J. Thiebot, S. Guillou, and J.-C. Brun-Cottan, "An optimisation method for determining permeability and effective stress relationships of consolidating cohesive sediment deposits," *Continental Shelf Research*, vol. 31, no. 10, pp. S117–S123, Jul. 2011. [Online]. Available: http://linkinghub.elsevier.com/retrieve/pii/S0278434310003675

[28] Thiebot, J., "Numerical modelling of the processes which govern the formation and the degradation of muddy massifs - application to the rance estuary and to the sèvre niortaise river banks," Ph.D. dissertation, Agro Paris Tech, Mar. 2008.

[29] L. A. Van, "Modélisation du transport des sédiments mixtes sable-vase et application à la morphodynamique de l?estuaire de la gironde," Ph.D. dissertation, Universite PARIS-EST, 2012.

[30] W. van Leussen, "The variability of settling velocities of suspended fine-grained sediment in the Ems estuary," *Journal of Sea Research*, vol. 41, no. 1-2, pp. 109–118, Mar. 1999. [Online]. Available: http://linkinghub.elsevier.com/retrieve/pii/S138511019800046X

[31] R. Whitehouse, Ed., *Dynamics of estuarine muds: a manual for practical applications*. London: Telford, 2000.

[32] J. Winterwerp, "On the flocculation and settling velocity of estuarine mud," *Continental Shelf Research*, vol. 22, no. 9, pp. 1339–1360, Jun. 2002. [Online]. Available: http://linkinghub.elsevier.com/retrieve/pii/S0278434302000109